

Hints Beyond Λ CDM from Barrow and Tsallis Holographic Dark Energy with GO cutoff

G. G. Luciano,^{1,*} A. Paliathanasis,^{2,3,4,†} G. Leon,^{4,2,‡} A. Sheykhi,^{5,6,§} and M. Motaghī⁵

¹*Departamento de Química, Física y Ciencias Ambientales y del Suelo,
Escuela Politécnica Superior – Lleida, Universidad de Lleida, Av. Jaume II, 69, 25001 Lleida, Spain*

²*Institute of Systems Science, Durban University of Technology, Durban 4000, South Africa*

³*National Institute for Theoretical and Computational Sciences (NITheCS), South Africa*

⁴*Departamento de Matemáticas, Universidad Católica del Norte,
Avda. Angamos 0610, Casilla 1280 Antofagasta, Chile*

⁵*Department of Physics, College of Science, Shiraz University, Shiraz 71454, Iran*

⁶*Biruni Observatory, College of Science, Shiraz University, Shiraz 71454, Iran*

(Dated: January 7, 2026)

Barrow and Tsallis Holographic Dark Energy (HDE) are two recent extensions of the standard HDE framework, obtained by introducing generalized entropy corrections through the Barrow and Tsallis formalisms. In this work, we examine the cosmological consequences of Barrow and Tsallis HDE implemented with the Granda-Oliveros (GO) infrared (IR) cutoff. After deriving the modified Friedmann equations within the thermodynamic-gravity conjecture, we study the background evolution in both non-interacting and interacting dark sector scenarios, emphasizing the role of the entropic parameter in shaping late-time dynamics. We then confront the model with state-of-the-art observations, including PantheonPlus and Union3 Type Ia supernovae, Cosmic Chronometers and DESI DR2 BAO measurements. Using Bayesian MCMC methods, we constrain the model parameters and compare the performance of BHDE with that of Λ CDM. Our results show that BHDE is compatible with current data and can exhibit a mild statistical preference over the concordance model for certain dataset combinations. Overall, the analysis underscores the relevance of generalized entropy frameworks in late-time cosmology and identifies Barrow-Tsallis holography with the GO cutoff as a competitive alternative to Λ CDM.

1. INTRODUCTION

The discovery of the accelerated expansion of the Universe at the end of the twentieth century fundamentally reshaped modern cosmology. Observations of distant type Ia supernovae revealed that cosmic expansion is speeding up [1, 2], implying the presence of an exotic energy component with strongly negative pressure. This mysterious constituent, commonly referred to as dark energy (DE), now represents the dominant contribution to the cosmic energy budget, yet its origin and physical nature remain largely unknown [3–7]. The cosmological constant Λ provides the simplest description of DE and yields an excellent fit to a broad range of cosmological observations. Nevertheless, the concordance Λ CDM model faces persistent theoretical and observational challenges [8–10], including the fine-tuning and coincidence problems, as well as tensions in the measurements of H_0 and σ_8 . These issues have motivated the exploration of dynamical DE scenarios, in which the equation of state (EoS) evolves with cosmic time [5, 11–16].

A particularly intriguing class of dynamical DE models arises from the holographic principle, which postulates that the number of degrees of freedom within a spatial region scales with its boundary area rather than its volume [17]. Applied to cosmology, this principle suggests that the DE density may depend on an infrared (IR) length scale L associated with the cosmological horizon [18, 19], leading to the holographic dark energy (HDE) density $\rho_{DE} \propto L^{-2}$.

The cosmological behaviour of HDE depends crucially on the choice of this cutoff. Several possibilities—such as the Hubble horizon, particle horizon and future event horizon—have been proposed, each leading to distinct physical and causal properties [19]. To address limitations associated with non-local cutoffs, Granda and Oliveros proposed a more general, local IR scale depending on both the Hubble rate and its time derivative [20, 21]

$$L = \left(\alpha H^2 + \beta \dot{H} \right)^{-1/2}, \quad (1)$$

*Electronic address: giuseppe.pegatano.luciano@udl.cat

†Electronic address: anpaliat@phys.uoa.gr

‡Electronic address: genly.leon@ucn.cl

§Electronic address: asheykhi@shirazu.ac.ir

where α and β are dimensionless parameters. This prescription avoids causality issues and naturally incorporates the dynamical evolution of the cosmic expansion.

The standard HDE model is based on the Bekenstein-Hawking entropy-area relation, which assumes the validity of semiclassical gravity. However, this assumption may break down in non-extensive or quantum-gravitational regimes. This possibility has prompted the construction of several generalized HDE models, obtained by replacing the conventional entropy with extended formulations such as Tsallis [22, 23], Renyi [24], Sharma-Mittal [25], and Kaniadakis [26] entropies [27]. A further layer of physical motivation for such extended approaches stems from the thermodynamic foundations of gravitational dynamics [28–37]. The well-established connection between the Friedmann equations and the first law of thermodynamics at the apparent horizon implies that any modification to the entropy-area relation induces corresponding corrections to the cosmological background equations. In this sense, generalized entropic frameworks predict a modified Friedmann dynamics, offering a rich setting to explore the interplay between horizon thermodynamics and cosmic acceleration [38–54].

Among the generalized entropic formulations introduced thus far, Barrow entropy has recently attracted significant attention. It introduces a quantum-gravitational deformation of the horizon geometry, leading to a fractal-like structure. The ensuing entropy takes the form [55]

$$S_\Delta = \left(\frac{A}{A_0} \right)^{1+\frac{\Delta}{2}}, \quad (2)$$

where A is the horizon area, $A_0 = 4G$ is the Planck area and Δ is a dimensionless parameter characterizing the degree of fractal deformation (we here adopt natural units). The classical Bekenstein-Hawking entropy is recovered for $\Delta = 0$, while $\Delta = 1$ represents a maximally deformed configuration. Although Barrow's original proposal focused on $\Delta > 0$, broader theoretical considerations suggest that negative values may also be physically meaningful [56, 57]. In fact, recent observational analyses indicate that mildly negative Δ could actually be favoured by cosmological data [58, 59]. Moreover, despite arising from conceptually distinct frameworks, the Barrow entropy (2) possesses the same functional form as the exponent ϵ in Tsallis entropy [60] under the correspondence $\Delta \rightarrow 2(\epsilon - 1)$. Consequently, although the subsequent analysis is developed within the Barrow framework, this formal equivalence ensures that the resulting cosmological dynamics and constraints can be straightforwardly extended to the Tsallis case as well.

The generalized entropy-area relation (2) has been shown to naturally modify the HDE density, leading to [61]

$$\rho_{DE} = CL^{\Delta-2}, \quad (3)$$

where C has dimensions $[L]^{-2-\Delta}$. In the limit $\Delta = 0$, the standard HDE form is recovered with $C = 3c^2M_p^2$, where c is a dimensionless constant and $M_p^2 = (8\pi G)^{-1}$ the reduced Planck mass. The resulting Barrow Holographic Dark Energy (BHDE) model has been extensively studied in various cosmological contexts. The inclusion of the Barrow exponent Δ enhances the compatibility of HDE with observational data, alleviating tensions related to the dark energy EoS and the Hubble parameter at low redshifts. It also enriches the dark-sector dynamics, enabling a smoother transition between cosmological epochs and a more flexible description of late-time acceleration [58, 59, 62–72].

Within the BHDE framework, several IR cutoffs have been considered [61–65]. Among these developments, the incorporation of the GO cutoff has been recently investigated [73, 74], showing that the combination of Barrow entropy with the dynamical GO scale yields a causally consistent and observationally viable model. This scenario predicts a delayed deceleration/acceleration transition and remains stable for specific parameter ranges, providing a cosmic evolution compatible with the latest data in both flat and non-flat geometries. Further studies have been recently conducted in this direction [75–77], where the BHDE model with the GO IR cutoff was explored from different perspectives. Specifically, Ref. [75] investigated the theoretical consistency of Barrow cosmology with the GO cutoff and confirmed the existence of a viable late-time accelerated phase. In Ref. [76], observational data were employed to constrain the model parameters and neutrino masses, showing that the BHDE-GO scenario remains compatible with current cosmological bounds. Moreover, Ref. [77] demonstrated that the same framework can significantly alleviate the Hubble tension. We will show that our results are in qualitative agreement with these works regarding the late-time acceleration of the BHDE-GO model, while extending the analysis by providing a complementary investigation of the cosmological dynamics, thereby further supporting the robustness and observational viability of the BHDE scenario.

Starting from the above premises, in this work we confront the BHDE model constructed with the GO IR cutoff with a broad set of current cosmological observations. In particular, we employ the Supernova PantheonPlus (PP) and Union3 (U3) compilations, the Observational Hubble Data (OHD) and the Baryon Acoustic Oscillation (BAO) measurements to constrain the model parameters and assess its phenomenological viability. The statistical performance of the BHDE scenario is then compared with that of the concordance Λ CDM model. Our analysis shows

that, for certain data combinations, the extended BHDE framework provides a better fit to the observations and exhibits a weak but non-negligible statistical preference over Λ CDM, while remaining fully consistent with the standard cosmological constraints.

The paper is structured as follows. In the next section, we review the derivation of the modified Friedmann equations in the context of Barrow cosmology, outlining the main theoretical ingredients relevant to the BHDE framework. In Sec. 3, we focus on the BHDE model with the GO cutoff, investigating both the non-interacting and interacting cases between the dark components. Observational analysis is conducted in Sec. 4, while conclusions and outlook are summarized in Sec. 5.

2. MODIFIED FRIEDMANN EQUATIONS FROM BARROW ENTROPY

We begin by revisiting the derivation of the modified Friedmann equations emerging from the Barrow entropy formalism. Within the thermodynamic approach to gravity, the cosmological dynamics can be obtained by applying the first law of thermodynamics to the apparent horizon, taking into account the entropy deformation proposed by Barrow [78].

Our analysis is performed within a spatially flat Friedmann-Lemaître-Robertson-Walker (FLRW) background, described by the metric

$$ds^2 = h_{\alpha\beta} dx^\alpha dx^\beta + \tilde{r}^2 (d\theta^2 + \sin^2 \theta d\phi^2), \quad (4)$$

where $\tilde{r} = a(t) r$, $x^0 = t$, $x^1 = r$, $h_{\alpha\beta} = \text{diag}(-1, a^2)$, and $a(t)$ denotes the time-dependent scale factor. We consider the apparent horizon as the effective boundary of the Universe, with radius $\tilde{r}_A = 1/H$, where the Hubble parameter $H = \dot{a}/a$ characterizes the rate of cosmic expansion, and the overdot denotes differentiation with respect to cosmic time [32, 34, 79]. This choice is compatible with both the first and second laws of thermodynamics.

Since the work done on the system is proportional to the change in volume (dV), the first law applied at the apparent horizon can be expressed as

$$dE = TdS + \mathcal{W}dV, \quad (5)$$

where the horizon temperature takes the Hawking-like expression [80]

$$T = -\frac{1}{2\pi\tilde{r}_A} \left(1 - \frac{\dot{\tilde{r}}_A}{2H\tilde{r}_A} \right), \quad (6)$$

in analogy with black hole thermodynamics [30, 79]. Furthermore, the work density \mathcal{W} , which arises from variations of the apparent horizon radius, is given by $\mathcal{W} = -\frac{1}{2} \text{Tr}(T^{\mu\nu}) = (\rho - p)/2$, where $T_{\mu\nu} = (\rho + p) u_\mu u_\nu + p g_{\mu\nu}$ is the energy-momentum tensor of the perfect fluid that fills the Universe. Here, ρ denotes the energy density, p is the isotropic pressure, u^μ is the four-velocity of a comoving observer satisfying $u^\mu u_\mu = -1$ and $g_{\mu\nu}$ represents the spacetime metric. The trace $\text{Tr}(T^{\mu\nu})$ is evaluated with respect to the induced metric on the (t, r) submanifold of the FLRW geometry.

By differentiating the total matter and energy $E = \rho V$ within a three-dimensional sphere of radius \tilde{r}_A , and using the continuity equation $\dot{\rho} + 3H(\rho + p) = 0$, we obtain

$$dE = 4\pi\tilde{r}_A^2 \rho d\tilde{r}_A - 4\pi H\tilde{r}_A^3 (\rho + p) dt. \quad (7)$$

On the other hand, differentiating the Barrow entropy expression (2) yields

$$dS = (2 + \Delta) \left(\frac{4\pi}{A_0} \right)^{1+\Delta/2} \tilde{r}_A^{1+\Delta} \dot{\tilde{r}}_A dt. \quad (8)$$

By substituting Eqs. (6), (7) and (8) into the first law of thermodynamics (5) and integrating, we finally obtain [74]

$$H^{2-\Delta} = \frac{8\pi G_{\text{eff}}}{3} \rho, \quad (9)$$

where we have expressed the horizon radius in terms the Hubble rate. Furthermore, we have defined the effective

gravitational constant

$$G_{\text{eff}} = \frac{A_0}{4} \left(\frac{2 - \Delta}{2 + \Delta} \right) \left(\frac{A_0}{4\pi} \right)^{\Delta/2}. \quad (10)$$

The relation (9) provides the modified Friedmann equation obtained from Barrow entropy. It is worth noting that in this formulation, the corrections arising from the modified entropy are incorporated through a redefinition of the gravitational constant. A conceptually different interpretation is provided in Ref. [44], where the Δ -dependent terms are treated as an additional contribution to the dark energy sector. Moreover, it is straightforward to verify that in the limit $\Delta \rightarrow 0$, the effective gravitational constant reduces to the standard value, $G_{\text{eff}} = G$, thereby recovering the conventional Friedmann dynamics.

3. BHDE WITH GO CUTOFF

We consider the BHDE model during an epoch in which the cosmic fluid contains both (pressureless) dark matter (DM) and DE. For later convenience, we rewrite Eq. (9) in the form

$$H^{2-\Delta} = \frac{1}{3M_{\text{eff}}^2} (\rho_m + \rho_{DE}), \quad (11)$$

where ρ_m is the matter energy density and $M_{\text{eff}}^2 \equiv (8\pi G_{\text{eff}})^{-1}$.

By combining the BHDE density (3) with the GO cutoff (1), the energy density can be written as

$$\rho_{DE} = 3M_{\text{eff}}^2 \left(\alpha H^2 + \beta \dot{H} \right)^{1-\Delta/2}, \quad (12)$$

where we have fixed the constant $C = 3M_{\text{eff}}^2$ (equivalent to setting $c^2 = 1$ in the standard normalization). In the limit $\Delta \rightarrow 0$, the results of [20, 21] are fully recovered, ensuring consistency with the standard GO HDE scenario.

3.1. Non-interacting (NI) case

We start by assuming that the dark sectors are conserved independently. In this case, the corresponding conservation equations read

$$\dot{\rho}_{DE} + 3H\rho_{DE}(1 + \omega_{DE}) = 0, \quad (13)$$

$$\dot{\rho}_m + 3H\rho_m = 0, \quad (14)$$

where $\omega_{DE} \equiv p_{DE}/\rho_{DE}$ is the EoS parameter of the DE component.

It is now convenient to introduce the effective critical energy density $\rho_{cr} = 3M_{\text{eff}}^2 H^{2-\Delta}$. In turn, the fractional energy densities of DM and DE are

$$\Omega_m \equiv \frac{\rho_m}{\rho_{cr}} = \frac{\rho_m}{3M_{\text{eff}}^2 H^{2-\Delta}}, \quad \Omega_{DE} \equiv \frac{\rho_{DE}}{\rho_{cr}} = \frac{\rho_{DE}}{3M_{\text{eff}}^2 H^{2-\Delta}}, \quad (15)$$

which enables us to rewrite the modified Friedmann equation (11) in the form $\Omega_m + \Omega_{DE} = 1$.

To explore the dynamics of the DE model throughout the history of the Universe, one must analyze the evolution of the DE density parameter Ω_{DE} . Using Eqs. (11) and (15) and some straightforward algebra, it can be shown that [74]

$$\frac{d\Omega_{DE}}{dz} = \frac{3(1 - \Omega_{DE})}{(1 + z)} \left[\frac{(\Delta - 2)}{3\beta} \left(\Omega_{DE}^{2/(2-\Delta)} - \alpha \right) - 1 \right], \quad (16)$$

where $z = 1/a - 1$ denotes the redshift variable (we set the present-day value of a to unity). The evolution of Ω_{DE} has been studied in [74]. Interestingly, the results indicate that for $z \gtrsim 0.6$, Ω_{DE} decreases with increasing values of Δ , whereas at lower redshifts the dependence on Δ becomes negligible. The EoS parameter and the deceleration

parameter are given by [74]

$$w_{DE} = \frac{1}{\Omega_{DE}} \left[\frac{(\Delta-2)}{3\beta} (\Omega_{DE}^{2/(2-\Delta)} - \alpha) - 1 \right], \quad (17)$$

$$q = -1 - \frac{\dot{H}}{H^2} = -1 - \frac{\Omega_{DE}^{2/(2-\Delta)} - \alpha}{\beta}. \quad (18)$$

3.2. Interacting (I) case

Next, we consider a FRW Universe composed of BHDE and DM, allowing for energy exchange between them. Since the fundamental nature of both dark components remains unknown, there is sufficient freedom to permit an interaction between these components [11]. Moreover, in [81] the interaction between DM and DE was thoroughly examined from a thermodynamic perspective.

In this scenario, the semi-conservation equations accounting for the interaction take the form

$$\dot{\rho}_{DE} + 3H\rho_{DE}(1 + \omega_{DE}) = -Q, \quad (19)$$

$$\dot{\rho}_m + 3H\rho_m = Q, \quad (20)$$

where Q parameterises the energy exchange between DE and DM. A variety of phenomenological ansätze for Q have been considered in the literature [82]. Following [74, 83], we set

$$Q = 3\gamma H(1+r)\rho_{DE}, \quad (21)$$

where $\gamma = b^2 > 0$ is a coupling constant and $r \equiv \rho_m/\rho_{DE}$ [83]. Since $Q > 0$ enters the DE continuity equation with a minus sign, the interaction term effectively describes an energy transfer from DE to DM.

The form (21) is largely used for several reasons. First, the factor H guarantees the correct dimensionality for a transfer rate and ties the strength of the interaction to the global expansion, while the additional term $(1+r)\rho_{DE} = \rho_{DE} + \rho_m$ ensures that the coupling is effectively proportional to the total energy density of the dark sector, thereby allowing the interaction to remain dynamically relevant both at early and late times. Moreover, the model retains phenomenological flexibility while involving only one additional dimensionless parameter, making it straightforward to implement in cosmological analyses and to constrain observationally [83].

Following calculations similar to those developed for the non-interacting model, it can be shown that the DE density obeys the generalized dynamics [74]

$$\frac{d\Omega_{DE}}{dz} = \frac{3}{(1+z)} \left\{ (1 - \Omega_{DE}) \left[\frac{(\Delta-2)}{3\beta} (\Omega_{DE}^{2/(2-\Delta)} - \alpha) - 1 \right] + \gamma \right\}, \quad (22)$$

which straightforwardly recovers Eq. (16) for $\gamma = 0$. Compared to the previous model, the effects of the interaction are manifested in a modified evolution of Ω_{DE} , which, for each z , is observed to decrease as γ decreases. It also shapes the evolution of the EoS parameter w_{DE} , which decreases as γ increases, reflecting the distinct ways in which the coupling influences each quantity. Notably, for sufficiently small values of γ , w_{DE} remains in the phantom regime at the present epoch [74].

For later convenience, we introduce a rescaling of the variables and rewrite Eq. (22) in the form

$$\frac{d\Omega_{DE}}{dz} = \frac{3}{(1+z)} \left\{ (1 - \Omega_{DE}) \left[(B\Omega_{DE}^{2/(2-\Delta)} - A) - 1 \right] + \gamma \right\}, \quad (23)$$

where $B = \frac{\Delta-2}{3\beta}$ and $A = \alpha B$. The EoS parameter and the deceleration parameter for the interacting case, are still given by Eqs. (17) and (18) [74], while in this case the evolutionary form of Ω_{DE} is governed by (23).

4. OBSERVATIONAL DATA ANALYSIS

In this section, we utilize different sets of observational data to place constraints on the free parameters of the BHDE model with the GO IR cutoff. By confronting the theoretical predictions with measurements from cosmological probes,

we aim to assess the viability of the model and quantify the allowed parameter space.

4.1. Observational Data

Let us first describe the specific datasets employed in this analysis:

- **PantheonPlus Supernovae (PP):** The PantheonPlus compilation includes a total of 1701 light curves corresponding to 1550 spectroscopically confirmed Type Ia supernovae. It provides observational measurements of the distance modulus μ^{obs} across the redshift interval $10^{-3} < z < 2.27$ [84]. The theoretical prediction for the distance modulus is given by

$$\mu^{\text{th}} = 5 \log_{10} D_L + 25, \quad (24)$$

where, under the assumption of a spatially flat FLRW metric, the luminosity distance is expressed as

$$D_L(z) = (1+z) \int_0^z \frac{dz'}{H(z')}. \quad (25)$$

In this work, we employ the PantheonPlus sample without incorporating the SH0ES Cepheid calibration.

- **Union3 Supernovae (U3):** The Union3 catalogue represents the most up-to-date supernova dataset, containing 2087 events within the same redshift interval as the PP compilation [85]. Of these, 1363 supernovae are common to both the Union3 and PantheonPlus catalogues.
- **Observational Hubble Data (OHD):** We utilize direct measurements of the Hubble parameter $H(z)$ derived from the Cosmic Chronometers (CC) method. These observations are model-independent, relying solely on the differential aging of passively evolving galaxies with synchronized stellar populations and homogeneous cosmic evolution [86]. Specifically, we employ 34 $H(z)$ data points spanning the redshift range $0.09 \leq z \leq 1.965$, as reported in [87] and the three new measurements from the analysis of the DESI DR1 data [88].
- **Baryon Acoustic Oscillations (BAO):** We incorporate the latest BAO measurements from the Dark Energy Spectroscopic Instrument (DESI) Data Release 2 (DR2) [89–91]. This dataset provides constraints on several cosmological distance ratios evaluated at seven distinct redshifts, namely:

$$\frac{D_M}{r_{\text{drag}}} = \frac{D_L}{(1+z)r_{\text{drag}}}, \quad \frac{D_V}{r_{\text{drag}}} = \frac{(zD_H D_M^2)^{1/3}}{r_{\text{drag}}}, \quad \frac{D_H}{r_{\text{drag}}} = \frac{1}{r_{\text{drag}} H(z)}, \quad (26)$$

where D_L is the luminosity distance and r_{drag} denotes the comoving sound horizon at the baryon-drag epoch. In our analysis, r_{drag} is treated as a free parameter.

4.2. Methodology

To perform the statistical inference, we employ the Bayesian analysis framework COBAYA¹ [92, 93], using a customized theoretical module coupled with its built-in Markov Chain Monte Carlo (MCMC) sampler [94, 95]. The resulting MCMC chains are post-processed and visualized using the GETDIST package² [96].

We analyze two distinct combinations of cosmological datasets, namely PP&OHD&BAO and U3&OHD&BAO. For each dataset configuration, the model parameters are estimated by maximizing the likelihood function, defined as $\mathcal{L}_{\text{max}} = \exp(-\frac{1}{2}\chi^2_{\text{min}})$, where the minimum chi-square value corresponds to the sum of the individual contributions from each dataset. For comparison purposes, the same statistical analysis is also carried out for the reference Λ CDM model.

Since the BHDE framework and the standard Λ CDM cosmology contain a different number of free parameters, a fair model comparison requires an information-based criterion. We therefore employ the Akaike Information Criterion

¹ <https://cobaya.readthedocs.io/>

² <https://getdist.readthedocs.io/>

Priors	BHDE	Λ CDM
H_0	[60, 80]	[60, 80]
Ω_{m0}	[0.01, 0.5]	[0.01, 0.5]
r_{drag}	[130, 160]	[130, 160]
Δ	[-1, 1]	—
A	[-5, 0]	—
\mathbf{B}	[-5, 0]	—
γ	[0, 1]	—

TABLE I: Priors adopted for the free parameters of the Λ CDM and BHDE models. For Λ CDM, the parameter set is $\{H_0, \Omega_{m0}, r_{\text{drag}}\}$, while for BHDE it includes $\{H_0, \Omega_{m0}, r_{\text{drag}}, \Delta, \alpha, \beta\}$ for the non-interacting model and $\{H_0, \Omega_{m0}, r_{\text{drag}}, \Delta, \alpha, \beta, \gamma\}$ for the interacting model.

(AIC) [97], defined as

$$\text{AIC} = \chi_{\min}^2 + 2\kappa, \quad (27)$$

where κ denotes the total number of independent parameters in the model. Lower AIC values correspond to a better balance between model complexity and goodness of fit.

To quantify the statistical preference between the two models, we compute the relative difference

$$\Delta\text{AIC} = \text{AIC}_{\text{BHDE}} - \text{AIC}_{\Lambda\text{CDM}}. \quad (28)$$

Because the BHDE framework includes more free parameters than the standard Λ CDM model (see Tab. I), the correction term in the AIC expression varies according to whether the BHDE model is interacting or not. In the non-interacting configuration, the additional degrees of freedom are $\{\Delta, \alpha, \beta\}$, corresponding to $\Delta\kappa = 3$. Therefore

$$\Delta\text{AIC}_{\text{NI}} = \chi_{\min}^2(\text{BHDE}_{\text{NI}}) - \chi_{\min}^2(\Lambda\text{CDM}) + 6. \quad (29)$$

On the other hand, in the interacting case an extra parameter associated with the coupling strength γ is introduced, giving $\Delta\kappa = 4$ and

$$\Delta\text{AIC}_{\text{I}} = \chi_{\min}^2(\text{BHDE}_{\text{I}}) - \chi_{\min}^2(\Lambda\text{CDM}) + 8. \quad (30)$$

Following Akaike's classification, models with $|\Delta\text{AIC}| < 2$ are statistically indistinguishable. Values in the range $2 < |\Delta\text{AIC}| < 6$ indicate weak evidence in favor of the model with the lower AIC, while $6 < |\Delta\text{AIC}| < 10$ corresponds to strong evidence. Finally, a difference exceeding 10 denotes decisive support for the model with the smaller AIC value.

To ensure consistency in the comparison and to mitigate any potential systematic bias, the Hubble expansion rate for the Λ CDM model has been computed numerically using the same procedure applied to the BHDE framework.

4.3. Results

We now present the results obtained from the analysis of the MCMC chains for the combined datasets PP&OHD&BAO and U3&OHD&BAO, for the two models under consideration, namely, the non-interacting (NI) BHDE and the interacting (I) BHDE.

4.3.1. Non-interacting case

The contour plots of the confidence regions for the best-fit parameters of the non-interacting BHDE model are displayed in Fig. 1. For the PP&OHD&BAO dataset, we obtain the posterior estimates $H_0 = 67.9_{-1.7}^{+1.7} \text{ km s}^{-1} \text{ Mpc}^{-1}$, $\Omega_{m0} = 0.358_{-0.02}^{+0.16}$, $r_{\text{drag}} = 147.5_{-3.5}^{+3.5} \text{ Mpc}$, $\Delta = -0.041_{-0.34}^{+0.01}$, $\alpha = 1.58_{-0.55}^{+0.23}$, and $\beta = 1.49_{-0.93}^{+0.49}$ (see Tab. II). This

model provides a slightly better fit to the data than Λ CDM, as indicated by $\chi^2_{\min} - \chi^2_{\Lambda, \min} = -4.27$. However, once the different numbers of degrees of freedom are taken into account, the Akaike information criterion shows that the two models are statistically equivalent, with $\Delta \text{AIC}_{\text{NI}} = +1.73$.

On the other hand, the introduction of the U3 catalogue, and for the dataset U3&OHD&BAO we find the posterior variables $H_0 = 66.2^{+1.7}_{-1.7}$, $\Omega_{m0} = 0.462^{+0.044}_{-0.044}$, $r_{\text{drag}} = 148.0^{+3.5}_{-3.5}$, $\Delta = -0.234^{+0.082}_{-0.093}$, $\alpha > 14.6$ and $\beta = 23^{+10}_{-7}$ (see Tab. II). Unlike the previous case, the data now show a weak preference for the BHDE model, with $\chi^2_{\min} - \chi^2_{\Lambda, \min} = -9.63$ and $\Delta \text{AIC}_{\text{NI}} = -3.63$.

It is worth commenting on the fact that the best-fit value of Δ turns out to be negative in both datasets. In the original Barrow proposal, positive values $\Delta > 0$ were introduced to model “spherelike”-type deformations of the horizon, leading to a surface with enhanced roughness. However, negative values of Δ correspond to “porous” or “spongy” geometries, which are also well motivated from the viewpoint of fractal geometry. Indeed, many classical fractal constructions possess effective anomalous dimensions below the topological one [56, 98]. Moreover, from the quantum field theory perspective, renormalization-group arguments allow for negative anomalous dimensions in several systems [57]. Even more significantly, negative logarithmic corrections to the Bekenstein–Hawking entropy - such as those obtained from the Cardy formula [99] - indicate that Δ may naturally take negative values.

Furthermore, we remark on the parameters α and β . According to [100], these parameters are expected to lie in the ranges $\alpha \in [0.7, 1.0]$ and $\beta \in [0.3, 0.9]$. For the PP&OHD&BAO dataset, our best-fit values are marginally consistent with these ranges within 1σ uncertainties. For the U3&OHD&BAO dataset, the estimates of α and β slightly exceed the expected ranges. These discrepancies can be attributed to the fact that the study of [100] focuses on redshifts $z \gtrsim 2$, whereas our datasets primarily probe lower-redshift regimes, in which the effective dynamics of the BHDE model may differ.

4.3.2. Interacting case

For the second model in our analysis, where interaction is included, the contour plots of the confidence regions for the best-fit parameters are shown in Fig. 2. We find for the PP&OHD&BAO dataset the posterior parameters $H_0 = 67.9^{+1.7}_{-1.7} \text{ km s}^{-1} \text{ Mpc}^{-1}$, $\Omega_{m0} = 0.418^{+0.079}_{-0.029}$, $r_{\text{drag}} = 147.5^{+3.4}_{-3.4} \text{ Mpc}$, $\Delta = -0.197^{+0.06}_{-0.16}$, $\alpha = 1.20^{+0.25}_{-0.56}$, $\beta = 1.31^{+0.29}_{-0.78}$, and $\gamma < 0.086$ (see Tab. II). In comparison with the Λ CDM model, the statistical parameter is $\chi^2_{\min} - \chi^2_{\Lambda, \min} = -4.27$, indicating that the BHDE models with and without interaction fit the data similarly. However, due to the different number of degrees of freedom, the data provide a weak preference for Λ CDM, since $\Delta \text{AIC}_{\text{I}} = +3.73$ in this case. Furthermore, the non-interacting model, which corresponds to $\gamma = 0$, lies within the 1σ posterior range.

For the dataset U3&OHD&BAO the analysis of the MCMC chains give $H_0 = 65.8^{+1.7}_{-1.7}$, $\Omega_{m0} = 0.480^{+0.039}_{-0.044}$, $r_{\text{drag}} = 148.1^{+3.5}_{-3.5}$, $\Delta = -0.260^{+0.083}_{-0.083}$, $\alpha = 17.0^{+12}_{-5.0}$, $\beta = 30^{+20}_{-8}$ and $\gamma < 0.127$. The two BHDE models fit the data with the same way, $\chi^2_{\min} - \chi^2_{\Lambda, \min} = -9.67$. Nevertheless, due to the different degrees of freedom, the interacting model is statistical equivalent with the Λ CDM, i.e. $\text{AIC} - \text{AIC}_{\Lambda} = -1.67$.

Analogously to the discussion presented above, the negative values of Δ are preferred. As for the parameters α and β , the estimates obtained from the PP&OHD&BAO dataset are broadly consistent with the ranges reported in [100], while those from the U3&OHD&BAO dataset show a mild tension, particularly for β . Finally, the interaction parameter γ is tightly constrained in both datasets, with upper limits compatible with typical values considered in the literature [101]. These results indicate that, while a non-zero interaction cannot be excluded, the data are also consistent with the non-interacting limit, showing that current observations place only weak constraints on the strength of the dark-sector coupling.

Moreover, from Fig. 1 we observe a correlation between the parameters α and β , which is present in both the non-interacting and interacting scenarios. This degeneracy is particularly evident when the U3 dataset is employed, whereas a mild tension between the two parameters emerges in the PP-based analysis. This behavior can be traced back to the different sensitivity of the two supernova compilations to late-time dark energy dynamics. Indeed, it is well known that the Union3 catalogue exhibits a stronger preference for a dynamical dark energy component compared to PantheonPlus, which in turn allows for a wider region of the (α, β) parameter space to be observationally viable. From a theoretical standpoint, the α - β degeneracy originates from the structure of the evolution equations (16) and (22), where the cosmological dynamics depends primarily on specific combinations of these parameters, such as the ratio α/β , rather than on their individual values. As a result, variations in α can be efficiently compensated by corresponding changes in β , leading to elongated confidence regions and, in the case of the U3&OHD&BAO dataset, to weak or absent upper bounds on these parameters. This highlights the intrinsic limitation of background data alone in fully breaking the degeneracy associated with the GO cutoff.

	H_0	Ω_{m0}	r_{drag}	Δ	α	β	γ	$\chi^2_{\min} - \chi^2_{\Lambda \min}$	$AIC - AIC_{\Lambda}$
Dataset: PP&OHD&BAO									
BHDE (NI)	$67.9^{+1.7}_{-1.7}$	$0.358^{+0.16}_{-0.02}$	$147.5^{+3.5}_{-3.5}$	$-0.041^{+0.01}_{-0.34}$	$1.58^{+0.23}_{-0.55}$	$1.49^{+0.49}_{-0.93}$	—	-4.27	+1.73
BHDE (I)	$67.9^{+1.7}_{-1.7}$	$0.418^{+0.079}_{-0.029}$	$147.5^{+3.4}_{-3.4}$	$-0.197^{+0.06}_{-0.16}$	$1.20^{+0.25}_{-0.56}$	$1.31^{+0.29}_{-0.78}$	< 0.086	-4.27	+3.73
Λ CDM	$68.5^{+1.6}_{-1.6}$	$0.31^{+0.011}_{-0.012}$	$147.1^{+3.4}_{-3.4}$	—	—	—	—	0	0
Dataset: U3&OHD&BAO									
BHDE (NI)	$66.2^{+1.7}_{-1.7}$	$0.462^{+0.044}_{-0.044}$	$148.0^{+3.5}_{-3.5}$	$-0.234^{+0.082}_{-0.093}$	> 14.6	23^{+10}_{-7}	—	-9.63	-3.63
BHDE (I)	$65.8^{+1.7}_{-1.7}$	$0.480^{+0.039}_{-0.044}$	$148.1^{+3.5}_{-3.5}$	$-0.260^{+0.083}_{-0.083}$	$17.0^{+12}_{-5.0}$	30^{+20}_{-8}	< 0.127	-9.67	-1.67
Λ CDM	$68.6^{+1.6}_{-1.6}$	$0.31^{+0.014}_{-0.014}$	$146.7^{+3.4}_{-3.4}$	—	—	—	—	0	0

TABLE II: Observational constraints on the BHDE and Λ CDM models.

4.4. Evolution of the cosmological parameters

It is also interesting to study the evolutions of the cosmological parameters such as Ω_{de} , w_{de} , q and v_s^2 as functions of redshift z for the allowed ranges of the model parameters derived in the previous subsection using data fitting. Let us consider the noninteracting and interacting cases, separately. Note that δ in these figures is the Barrow exponent, namely $\delta = \Delta$.

4.4.1. Noninteracting case

For the noninteracting case, the evolutions of Ω_{de} , w_{de} , q are governed by Eqs. (16), (17) and (18). In Figs. (3)-(5), we have plotted the behaviour of these parameters against z . From these figures, we observe that the behaviour of the cosmological parameters are compatible with recent observation for the allowed ranges of α , β and δ . Here we have taken the values of these parameters in the ranges given by data fitting.

4.4.2. Interacting case

For the interacting case, the dynamics of Ω_{de} is followed by Eq. (23), while the evolutions of w_{de} and q are still governed by Eqs. (17) and (18). In Figs. (6)-(8), we have plotted the behaviour of these parameters against z . Again, we see that the behaviour of the parameters are compatible with recent observations.

Finally, we plot the evolution of squared sound speed (v_s^2) to verify the instability of the model through a semi-Newtonian approach. Here we only present two figures for some allowed ranges of the model parameters. The details of this study can be found in [74].

5. CONCLUSIONS

In this work, we have explored the cosmological consequences of Barrow and Tsallis HDE implemented with the GO-IR cutoff. By deriving the modified Friedmann equations that follow from the Barrow entropy deformation and analyzing both non-interacting and interacting dark sector configurations, we have investigated how the entropic parameter Δ influences the late-time expansion history. Confronting the theoretical predictions with several state-of-the-art observational datasets-including Type Ia supernovae from PantheonPlus and Union3, Hubble parameter measurements from Cosmic Chronometers and BAO distance indicators from DESI DR2-we obtained tight constraints on the BHDE parameter space through a Bayesian MCMC analysis.

Our results indicate that the BHDE scenario provides a robust description of the late-time Universe and remains fully compatible with current observations. Overall, the model provides a fit to the data comparable to, and in some cases slightly better than, that of Λ CDM, although the concordance model still retains a marginal statistical preference according to the Akaike Information Criterion once differences in model complexity are taken into account. This trend is, however, reversed when the U3&OHD&BAO dataset is considered. In this case the non-interacting

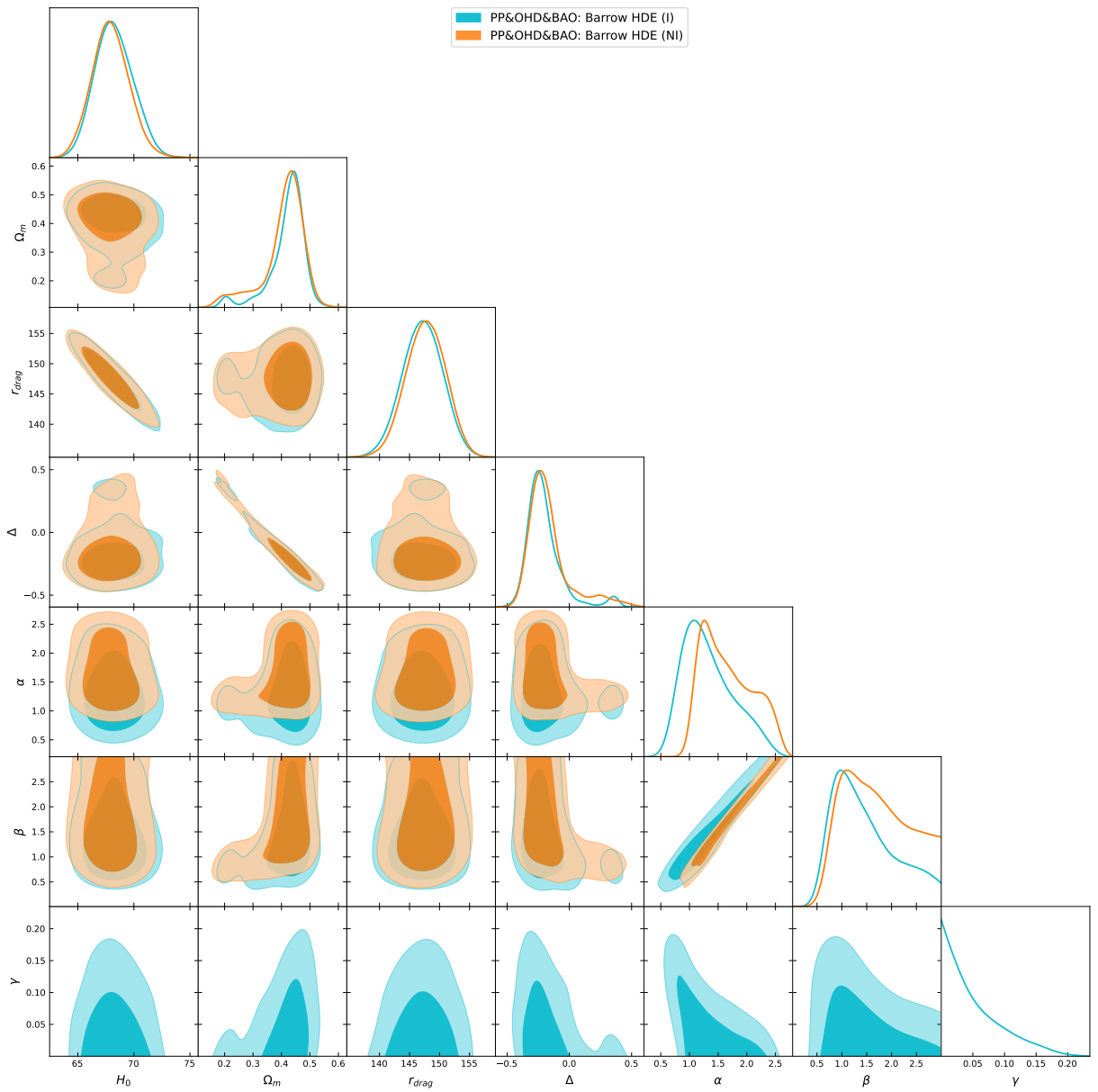


FIG. 1: Confidence space for the posterior parameters for the non-interacting BHDE model.

BHDE scenario shows a weak statistical preference over Λ CDM, while the interacting version becomes statistically equivalent to the concordance model.

Notably, our analysis favors slightly negative values of the Barrow entropic index Δ , in agreement with recent independent studies and with the theoretical allowance for anomalous fractal deformations of the horizon geometry [56–59]. These findings reinforce the relevance of generalized entropy frameworks as promising extensions of HDE, offering a richer phenomenology while preserving consistency with late-time cosmological probes. It is worth stressing that, although our analysis has been carried out explicitly within the Barrow entropy framework, the results straightforwardly extend to the Tsallis HDE scenario. Indeed, as emphasized in the Introduction, Barrow and Tsallis entropies share the same functional dependence on the horizon area, provided the correspondence $\Delta \rightarrow 2(\epsilon - 1)$ is applied. Consequently, the cosmological dynamics and observational constraints derived in this work are equally valid for Tsallis HDE upon a simple reparametrization of the entropic index. In this light, the preference for slightly negative values of the Barrow parameter Δ translates into $\epsilon < 1$ in the Tsallis formulation, corresponding to a sub-extensive scaling of the Tsallis entropy. This regime is well motivated within non-extensive statistical mechanics and further supports the physical viability of generalized entropy-based holographic dark energy models (see, e.g. [102]).

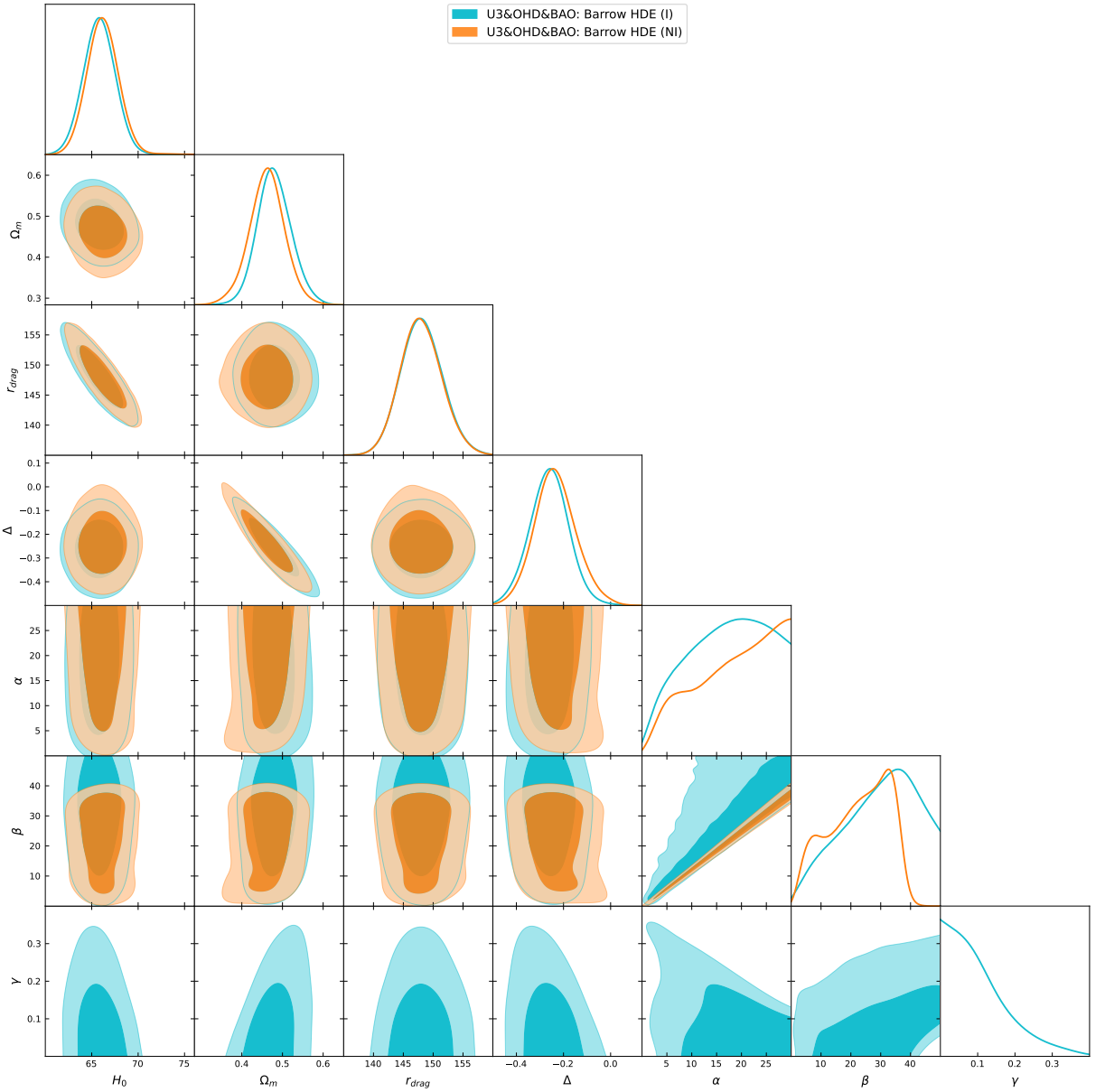


FIG. 2: Confidence space for the best-fit parameters for the interacting BHDE model.

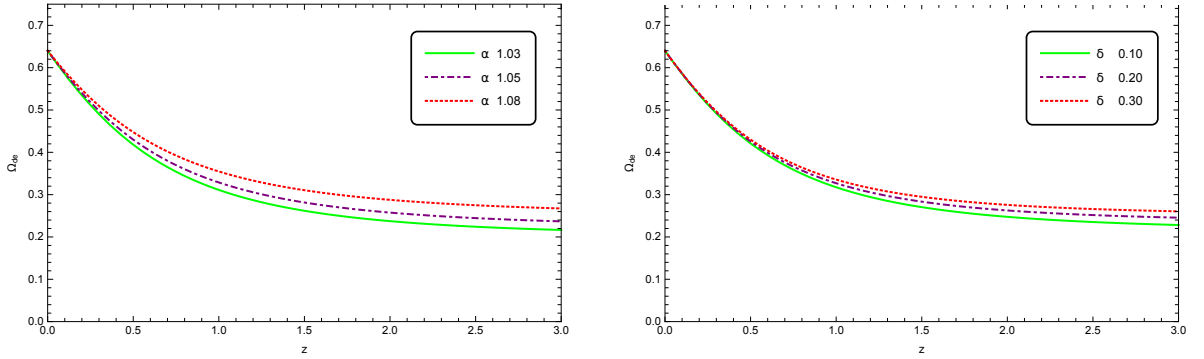


FIG. 3: Evolution of Ω_{de} against z for BHDE in a flat cosmology for $\Omega_{m,0} = 0.36$ and $\beta = 0.56$. In the left panel $\delta = -0.04$, while in the right panel $\alpha = 1.03$.

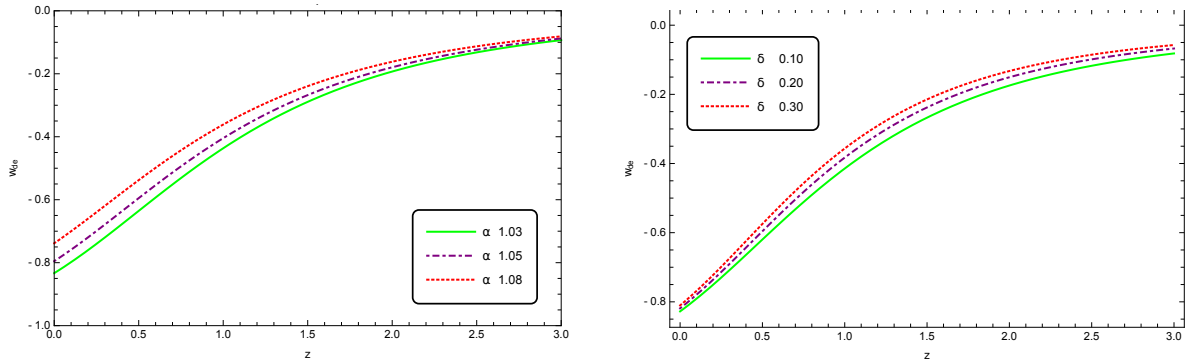


FIG. 4: Evolution of w_{de} against z for BHDE in a flat cosmology for $\Omega_{m,0} = 0.36$ and $\beta = 0.56$. In the left panel $\delta = -0.04$, while in the right panel $\alpha = 1.03$.

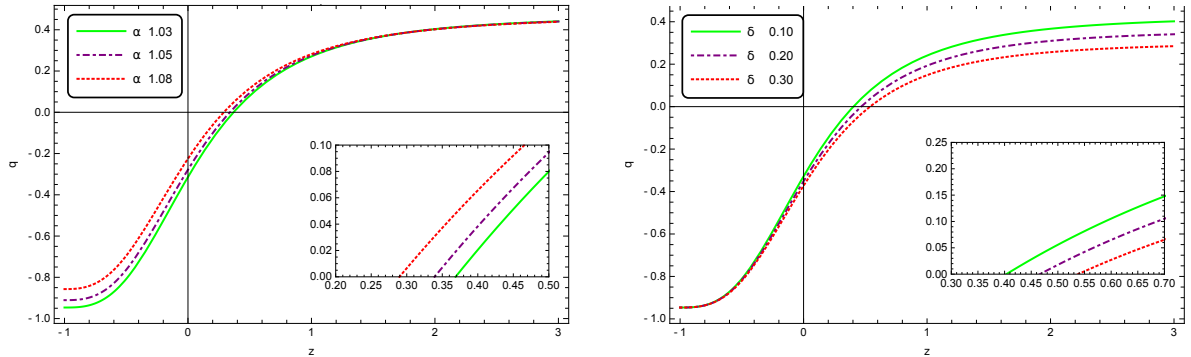


FIG. 5: Evolution of the deceleration parameter q against z for BHDE in a flat cosmology for $\Omega_{m,0} = 0.36$ and $\beta = 0.56$. In the left panel $\delta = -0.04$, while in the right panel $\alpha = 1.03$.

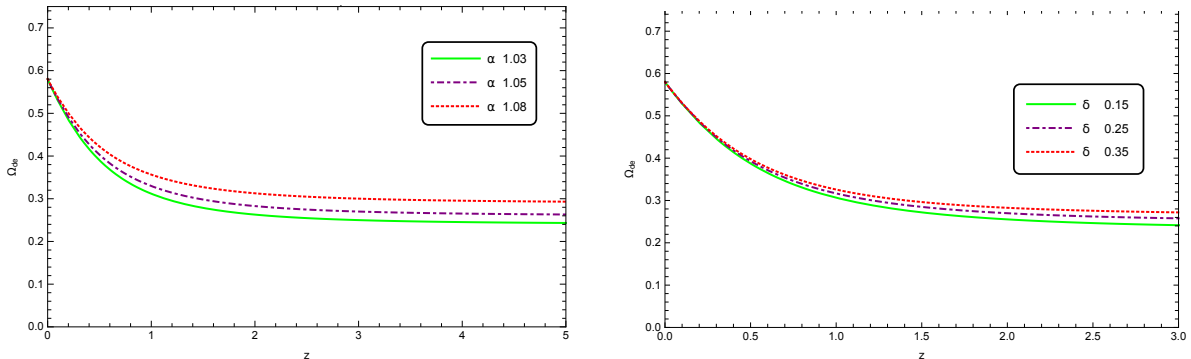


FIG. 6: Evolution of Ω_{de} against z for interacting BHDE in a flat cosmology for $\Omega_{m,0} = 0.42$, $\gamma = 0.086$ and $\beta = 0.56$. In the left panel $\delta = -0.2$, while in the right panel $\alpha = 1.03$.

for a review of recent cosmological bounds on Tsallis parameter).

Several avenues merit further exploration. A natural extension of this work is the study of BHDE at the perturbative level, focusing on structure growth and, in particular, the σ_8 tension. Such analyses would allow one to assess whether entropic modifications can simultaneously describe both the expansion history and the clustering properties of matter. Incorporating CMB temperature and polarization spectra would further strengthen the constraints and test the consistency of the model across cosmic epochs. Additionally, the framework provides an intriguing context for examining the Hubble tension. Indeed, generalized entropy corrections may introduce subtle modifications to the late-time expansion rate, and future work could investigate whether BHDE can offer a physically motivated route toward reconciling high-redshift and low-redshift determinations of H_0 .

Taken together, our results highlight Barrow and Tsallis HDE models with the GO cutoff as viable and competitive

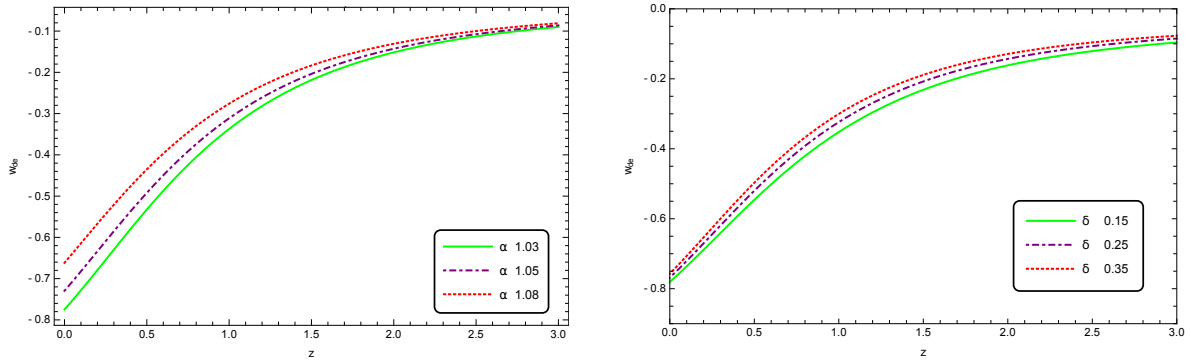


FIG. 7: Evolution of w_{de} against z for interacting BHDE in a flat cosmology for $\Omega_{m,0} = 0.42$, $\gamma = 0.086$ and $\beta = 0.56$. In the left panel $\delta = -0.2$, while in the right panel $\alpha = 1.03$.

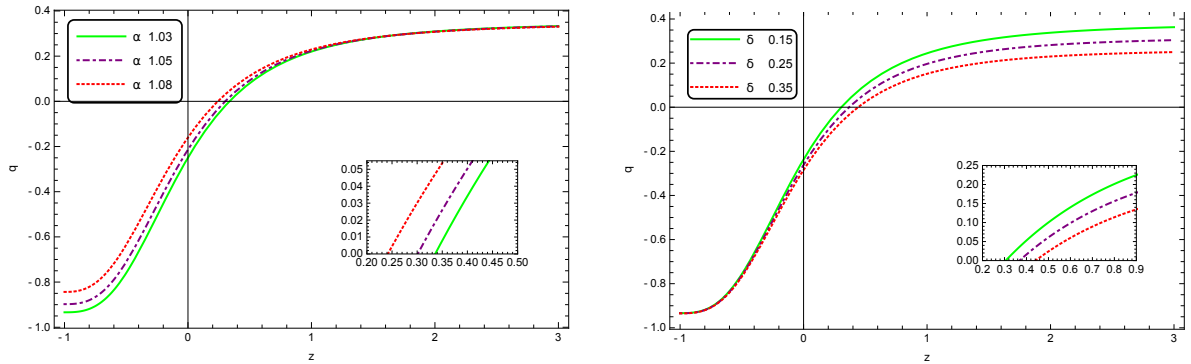


FIG. 8: Evolution of the deceleration parameter q against z for interacting BHDE in a flat cosmology for $\Omega_{m,0} = 0.42$, $\gamma = 0.086$ and $\beta = 0.56$. In the left panel $\delta = -0.2$, while in the right panel $\alpha = 1.03$.

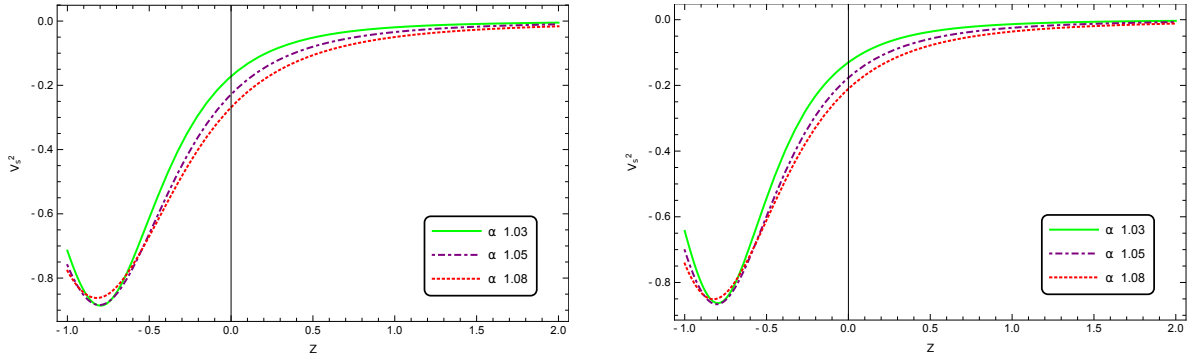


FIG. 9: Evolution of v_s^2 against z for BHDE in a flat cosmology for $\Omega_{m,0} = 0.36$, $\delta = -0.04$ and $\beta = 0.56$. Left panel for noninteracting case while right panel for interacting case with $\gamma = 0.086$.

extension of the standard dark energy paradigm. A comprehensive investigation of its perturbative predictions, early-Universe imprints and implications for cosmological tensions will be essential for fully assessing the role of generalized entropy in the gravitational and cosmological sectors. These directions will be the subject of future work.

Acknowledgments

The research of GGL is supported by the postdoctoral fellowship program of the University of Lleida. GGL gratefully acknowledges the contribution of the LISA Cosmology Working Group (CosWG), as well as support from the COST Actions CA21136 - *Addressing observational tensions in cosmology with systematics and fundamental physics (CosmoVerse)* - CA23130, *Bridging high and low energies in search of quantum gravity (BridgeQG)* and

CA21106 - *COSMIC WISPers in the Dark Universe: Theory, astrophysics and experiments (CosmicWISPers)*. AP & GL thank the support of VRIDT through Resolución VRIDT No. 096/2022 and Resolución VRIDT No. 098/2022. Part of this study was supported by FONDECYT 1240514.

[1] A. G. Riess et al. (Supernova Search Team), *Astron. J.* **116**, 1009 (1998), astro-ph/9805201.

[2] S. Perlmutter et al. (Supernova Cosmology Project), *Astrophys. J.* **517**, 565 (1999), astro-ph/9812133.

[3] P. Bull et al., *Phys. Dark Univ.* **12**, 56 (2016), 1512.05356.

[4] P. J. E. Peebles and B. Ratra, *Rev. Mod. Phys.* **75**, 559 (2003), astro-ph/0207347.

[5] E. J. Copeland, M. Sami, and S. Tsujikawa, *Int. J. Mod. Phys. D* **15**, 1753 (2006), hep-th/0603057.

[6] J. Frieman, M. Turner, and D. Huterer, *Ann. Rev. Astron. Astrophys.* **46**, 385 (2008), 0803.0982.

[7] K. Bamba, S. Capozziello, S. Nojiri, and S. D. Odintsov, *Astrophys. Space Sci.* **342**, 155 (2012), 1205.3421.

[8] L. Perivolaropoulos and F. Skara, *New Astron. Rev.* **95**, 101659 (2022), 2105.05208.

[9] Y. Akrami et al. (CANTATA), *Modified Gravity and Cosmology. An Update by the CANTATA Network* (Springer, 2021), ISBN 978-3-030-83714-3, 978-3-030-83717-4, 978-3-030-83715-0, 2105.12582.

[10] E. Di Valentino, O. Mena, S. Pan, L. Visinelli, W. Yang, A. Melchiorri, D. F. Mota, A. G. Riess, and J. Silk, *Class. Quant. Grav.* **38**, 153001 (2021), 2103.01183.

[11] C. Wetterich, *Nucl. Phys. B* **302**, 668 (1988), 1711.03844.

[12] S. Tsujikawa, *Class. Quant. Grav.* **30**, 214003 (2013), 1304.1961.

[13] I. Antoniadis, P. O. Mazur, and E. Mottola, *New J. Phys.* **9**, 11 (2007), gr-qc/0612068.

[14] S. Pan, W. Yang, and A. Paliathanasis, *Eur. Phys. J. C* **80**, 274 (2020), 1902.07108.

[15] M. Najafi, S. Pan, E. Di Valentino, and J. T. Firouzjaee, *Phys. Dark Univ.* **45**, 101539 (2024), 2407.14939.

[16] M. Rezaei, S. Pan, W. Yang, and D. F. Mota (2025), 2510.09766.

[17] G. 't Hooft, *Conf. Proc. C* **930308**, 284 (1993), gr-qc/9310026.

[18] M. Li, *Phys. Lett. B* **603**, 1 (2004), hep-th/0403127.

[19] S. Wang, Y. Wang, and M. Li, *Phys. Rept.* **696**, 1 (2017), 1612.00345.

[20] L. N. Granda and A. Oliveros, *Phys. Lett. B* **669**, 275 (2008), 0810.3149.

[21] L. N. Granda and A. Oliveros, *Phys. Lett. B* **671**, 199 (2009), 0810.3663.

[22] M. Tavayef, A. Sheykhi, K. Bamba, and H. Moradpour, *Phys. Lett. B* **781**, 195 (2018), 1804.02983.

[23] E. N. Saridakis, K. Bamba, R. Myrzakulov, and F. K. Anagnostopoulos, *JCAP* **12**, 012 (2018), 1806.01301.

[24] H. Moradpour, S. A. Moosavi, I. P. Lobo, J. P. Morais Graça, A. Jawad, and I. G. Salako, *Eur. Phys. J. C* **78**, 829 (2018), 1803.02195.

[25] A. Sayahian Jahromi, S. A. Moosavi, H. Moradpour, J. P. Morais Graça, I. P. Lobo, I. G. Salako, and A. Jawad, *Phys. Lett. B* **780**, 21 (2018), 1802.07722.

[26] N. Drepou, A. Lymperis, E. N. Saridakis, and K. Yesmakhanova, *Eur. Phys. J. C* **82**, 449 (2022), 2109.09181.

[27] S. Nojiri, S. D. Odintsov, and T. Paul, *Symmetry* **13**, 928 (2021), 2105.08438.

[28] T. Jacobson, *Phys. Rev. Lett.* **75**, 1260 (1995), gr-qc/9504004.

[29] T. Padmanabhan, *Phys. Rept.* **406**, 49 (2005), gr-qc/0311036.

[30] T. Padmanabhan, *Rept. Prog. Phys.* **73**, 046901 (2010), 0911.5004.

[31] A. Paranjape, S. Sarkar, and T. Padmanabhan, *Phys. Rev. D* **74**, 104015 (2006), hep-th/0607240.

[32] A. V. Frolov and L. Kofman, *JCAP* **05**, 009 (2003), hep-th/0212327.

[33] B. Wang, E. Abdalla, and R.-K. Su, *Phys. Lett. B* **503**, 394 (2001), hep-th/0101073.

[34] R.-G. Cai and S. P. Kim, *JHEP* **02**, 050 (2005), hep-th/0501055.

[35] R.-G. Cai and L.-M. Cao, *Nucl. Phys. B* **785**, 135 (2007), hep-th/0612144.

[36] R.-G. Cai, *Prog. Theor. Phys. Suppl.* **172**, 100 (2008), 0712.2142.

[37] R.-G. Cai, *Phys. Lett. B* **657**, 228 (2007), 0707.4049.

[38] J. D. Barrow, S. Basilakos, and E. N. Saridakis, *Phys. Lett. B* **815**, 136134 (2021), 2010.00986.

[39] G. Leon, J. Magaña, A. Hernández-Almada, M. A. García-Aspeitia, T. Verdugo, and V. Motta, *JCAP* **12**, 032 (2021), 2108.10998.

[40] M. Asghari and A. Sheykhi, *Eur. Phys. J. C* **82**, 388 (2022), 2110.00059.

[41] G. G. Luciano and E. N. Saridakis, *Eur. Phys. J. C* **82**, 558 (2022), 2203.12010.

[42] N. Myrzakulov, S. H. Shekh, and A. Pradhan, *Phys. Dark Univ.* **47**, 101790 (2025), 2411.18911.

[43] A. Lymperis and E. N. Saridakis, *Eur. Phys. J. C* **78**, 993 (2018), 1806.04614.

[44] E. N. Saridakis, *JCAP* **07**, 031 (2020), 2006.01105.

[45] S. Nojiri, S. D. Odintsov, and E. N. Saridakis, *Eur. Phys. J. C* **79**, 242 (2019), 1903.03098.

[46] A. Hernández-Almada, G. Leon, J. Magaña, M. A. García-Aspeitia, V. Motta, E. N. Saridakis, K. Yesmakhanova, and A. D. Millano, *Mon. Not. Roy. Astron. Soc.* **512**, 5122 (2022), 2112.04615.

[47] M. Dheepika, H. B. V. T., and T. K. Mathew, *Phys. Scripta* **99**, 015014 (2024), 2211.14039.

[48] P. Jizba, G. Lambiase, G. G. Luciano, and L. Petrucciello, *Phys. Rev. D* **105**, L121501 (2022), 2201.07919.

[49] G. Lambiase, G. G. Luciano, and A. Sheykhi, *Eur. Phys. J. C* **83**, 936 (2023), 2307.04027.

[50] P. Jizba, G. Lambiase, G. G. Luciano, and L. Mastrototaro, *Eur. Phys. J. C* **84**, 1076 (2024), 2403.09797.

[51] E. Ebrahimi and A. Sheykhi, Phys. Dark Univ. **45**, 101518 (2024), 2405.13096.

[52] S. Nojiri, S. D. Odintsov, T. Paul, and S. SenGupta (2025), 2503.19056.

[53] R. D'Agostino, Phys. Rev. D **99**, 103524 (2019), 1903.03836.

[54] R. D'Agostino and G. G. Luciano, Phys. Lett. B **857**, 138987 (2024), 2408.13638.

[55] J. D. Barrow, Phys. Lett. B **808**, 135643 (2020), 2004.09444.

[56] H. P. Tang, J. Z. Wang, J. L. Zhu, Q. B. Ao, J. Y. Wang, B. J. Yang, and Y. N. Li, Powder Technology **217**, 383 (2012).

[57] E. Dagotto, A. Kocic, and J. B. Kogut, Phys. Lett. B **237**, 268 (1990).

[58] G. G. Luciano, A. Paliathanasis, and E. N. Saridakis, JHEAp **49**, 100427 (2026), 2506.03019.

[59] G. G. Luciano, A. Paliathanasis, and E. N. Saridakis, JCAP **09**, 013 (2025), 2504.12205.

[60] C. Tsallis and L. J. L. Cirto, Eur. Phys. J. C **73**, 2487 (2013).

[61] E. N. Saridakis, Phys. Rev. D **102**, 123525 (2020), 2005.04115.

[62] F. K. Anagnostopoulos, S. Basilakos, and E. N. Saridakis, Eur. Phys. J. C **80**, 826 (2020), 2005.10302.

[63] M. P. Dabrowski and V. Salzano, Phys. Rev. D **102**, 064047 (2020), 2009.08306.

[64] S. Srivastava and U. K. Sharma, Int. J. Geom. Meth. Mod. Phys. **18**, 2150014 (2021), 2010.09439.

[65] P. Adhikary, S. Das, S. Basilakos, and E. N. Saridakis, Phys. Rev. D **104**, 123519 (2021), 2104.13118.

[66] S. Nojiri, S. D. Odintsov, and T. Paul, Phys. Lett. B **825**, 136844 (2022), 2112.10159.

[67] G. G. Luciano and J. Giné, Phys. Dark Univ. **41**, 101256 (2023), 2210.09755.

[68] A. Sheykhi and M. S. Hamedan, Entropy **25**, 569 (2023), 2211.00088.

[69] G. G. Luciano, Phys. Rev. D **106**, 083530 (2022), 2210.06320.

[70] G. G. Luciano, Phys. Dark Univ. **41**, 101237 (2023), 2301.12488.

[71] J.-X. Li and S. Wang, JCAP **07**, 047 (2025), 2412.09064.

[72] S. Basilakos, A. Lymperis, M. Petronikolou, and E. N. Saridakis (2023), 2312.15767.

[73] A. Oliveros, M. A. Sabogal, and M. A. Acero, Eur. Phys. J. Plus **137**, 783 (2022), 2203.14464.

[74] M. Motaghi, A. Sheykhi, and E. Ebrahimi, Phys. Dark Univ. **46**, 101710 (2024), 2407.21074.

[75] M. Mahmoudifard, M. Yarahmadi, and A. Salehi, Phys. Dark Univ. **48**, 101942 (2025).

[76] M. Mahmoudifard, A. Salehi, and R. Sepahvand, Eur. Phys. J. C **84**, 1099 (2024).

[77] M. Yarahmadi and A. Salehi, Mon. Not. Roy. Astron. Soc. **534**, 3055 (2024).

[78] A. Sheykhi, Phys. Rev. D **103**, 123503 (2021), 2102.06550.

[79] R.-G. Cai, L.-M. Cao, Y.-P. Hu, and N. Ohta, Phys. Rev. D **80**, 104016 (2009), 0910.2387.

[80] S. W. Hawking, Commun. Math. Phys. **43**, 199 (1975), [Erratum: Commun. Math. Phys. 46, 206 (1976)].

[81] S. H. Pereira and J. F. Jesus, Phys. Rev. D **79**, 043517 (2009), 0811.0099.

[82] B. Wang, E. Abdalla, F. Atrio-Barandela, and D. Pavon, Rept. Prog. Phys. **79**, 096901 (2016), 1603.08299.

[83] D. Pavon and W. Zimdahl, Phys. Lett. B **628**, 206 (2005), gr-qc/0505020.

[84] D. Scolnic et al., Astrophys. J. **938**, 113 (2022), 2112.03863.

[85] D. Rubin et al. (2023), 2311.12098.

[86] J.-J. Wei, F. Melia, and X.-F. Wu, Astrophys. J. **835**, 270 (2017), 1612.08491.

[87] S. Vagnozzi, A. Loeb, and M. Moresco, Astrophys. J. **908**, 84 (2021), 2011.11645.

[88] S. I. Loubser (2025), 2511.02730.

[89] M. Abdul Karim et al. (DESI) (2025), 2503.14739.

[90] M. Abdul Karim et al. (DESI) (2025), 2503.14738.

[91] K. Lodha et al. (DESI) (2025), 2503.14743.

[92] J. Torrado and A. Lewis, Astrophysics Source Code Library, (2019), ascl:1910.019.

[93] J. Torrado and A. Lewis, JCAP **05**, 057 (2021), 2005.05290.

[94] A. Lewis and S. Bridle, Phys. Rev. D **66**, 103511 (2002), astro-ph/0205436.

[95] A. Lewis, Phys. Rev. D **87**, 103529 (2013), 1304.4473.

[96] A. Lewis, JCAP **08**, 025 (2025), 1910.13970.

[97] H. Akaike, IEEE Trans. Automatic Control **19**, 716 (1974).

[98] P. Xu and B. Yu, Advances in Water Resources **31**, 74 (2008).

[99] S. Carlip, Class. Quant. Grav. **17**, 4175 (2000), gr-qc/0005017.

[100] M. T. Manoharan, Eur. Phys. J. C **84**, 552 (2024).

[101] D.-M. Xia and S. Wang, Mon. Not. Roy. Astron. Soc. **463**, 952 (2016), 1608.04545.

[102] G. G. Luciano and J. Gine, Phys. Lett. B **833**, 137352 (2022), 2204.02723.